

Intelligent Neural Network-Based Fast Power System Harmonic Detection

Hsiung Cheng Lin

Abstract—Nowadays, harmonic distortion in power systems is attracting significant attention. Traditional technical tools for harmonic distortion analysis using either fast Fourier transform or discrete Fourier transform are, however, susceptible to the presence of noise in the distorted signals. Harmonic detection by using Fourier transformation also requires input data for more than one cycle of the current waveform and requires time for the analysis in the next coming cycle. In this paper, an alternative method using neural network algorithm has achieved satisfactory results for fast and precise harmonic detection in noisy environments by providing only 1/2 cycle sampled values of distorted waveforms to neural network. Sensitivity considerations are conducted to determine the key factors affecting the performance efficiency of the proposed model to reach the lowest errors of testing patterns.

Index Terms—Artificial neural network (ANN), discrete Fourier transform (DFT), fast Fourier transform (FFT), power system harmonic, total harmonic distortion (THD).

I. INTRODUCTION

THE INCREASING application of power electronic facilities in the industrial environment has led to serious concerns about source line pollution and the resulting impacts on system equipment and power distribution systems. Power systems, in the presence of electronic equipment, can produce not only integer, but also subinteger and noninteger harmonics in the power signal waveforms. Power converters, specifically, are responsible for a disproportionate amount of the harmonics troubling power systems today [1]. Converters are used in variable-speed drives, power supplies, and uninterruptible power supply (UPS) systems; the term converter can refer to rectifiers, inverters, and cycloconverters. Arc furnaces are another significant source of harmonics. Harmonics in power systems can be the source of a variety of unwelcome effects, for examples, signal interference, overvoltages, data loss, and circuit breaker failure, as well as equipment heating, malfunction, and damage. Harmonics have been also known to be responsible for noise on both telephone and data transmission lines, and they can induce malfunction of relays and meters. Harmonic current components that react as the carrier signals in a particular system can interfere with the use of the carrier signals [2]. Electronic

devices are particularly vulnerable; huge increases in computer data loss, up to ten times the previous amount of data loss, were recorded after one installation of harmonics-producing equipment [3]. Harmonics can also cause excessive heating in transformers and capacitors, resulting in shortened life or failure. Rotor heating and pulsating output torque caused by harmonics can result in excessive motor heating and inefficiency.

Consequently, active power filters (APFs) have been used as an effective way to compensate harmonic components in nonlinear loads. APFs basically work by detecting the harmonic components from the distorted signals and injecting these harmonic current components with a current of the same magnitude but opposite phase into the power system to eliminate these harmonics. Active filter topologies have been recently discussed in many papers [4]–[6]. A comprehensive study of practical topologies was given by Akagi in [7]. Obviously, fast and precise harmonic detection is one of the key factors to design APFs. It is, therefore, crucial to identify the harmonic components, determine their magnitudes and phase angles, and generate an appropriate injection current to reduce harmonics to an acceptable level. Recently, one of the important literatures is that a multi-stage adaptive filtering system to generate the current reference was introduced by Valivita and Ovaska [8]. Its filter structure combining a low-pass prefilter and an adaptive predictive filter is capable of extracting the fundamental sinusoid active current from the distorted waveform in case of noisy disturbance. It is, however, the noise must be attenuated to considerably smaller using adaptive predictive filter. Besides, the Current Magnitude Estimator and Lagrange Interpolator involved in the proposed scheme made this approach more complex.

Alternatively, the simplest way to identify harmonics and generate the harmonic current is to use discrete Fourier transform (DFT) or fast Fourier transform (FFT). Although it has wide applications, the DFT or FFT has certain limitations in harmonic analysis [9]–[12]. Circumstances are encountered in practice for which the DFT (or FFT) cannot be relied on to achieve valid harmonic component identification. These include where there are existing noise signals which are not integer multiples of the supply frequency [2]. High-frequency noise beyond 500 Hz can be easily eliminated using low-pass filters before applying Fourier transform [13]. However, it is still troublesome to remove the possible lower frequency noise that may exist in the distorted waveform.

Presently, neural network has received special attention from the researchers because of its simplicity, learning and generalization ability, and it has been applied in the field of engineering, such as in harmonic detection since early 1900s [14]–[19]. These proposed methods, however, have some drawbacks like only lower frequency harmonic detection

Manuscript received December 15, 2004; revised June 4, 2005. Abstract published on the Internet November 30, 2006. This work was supported in part by the National Science Council of the Republic of China, Taiwan, under Grant NSC 93-2213-E-270-015.

The author is with the Department of Automation Engineering, Chienkuo Technology University, Chang Hua City 500, Taiwan (e-mail: hclin@cc.ctu.edu.tw).

Color versions of one or more of the figures in this paper are available online at <http://ieeexplore.ieee.org>.

Digital Object Identifier 10.1109/TIE.2006.888685

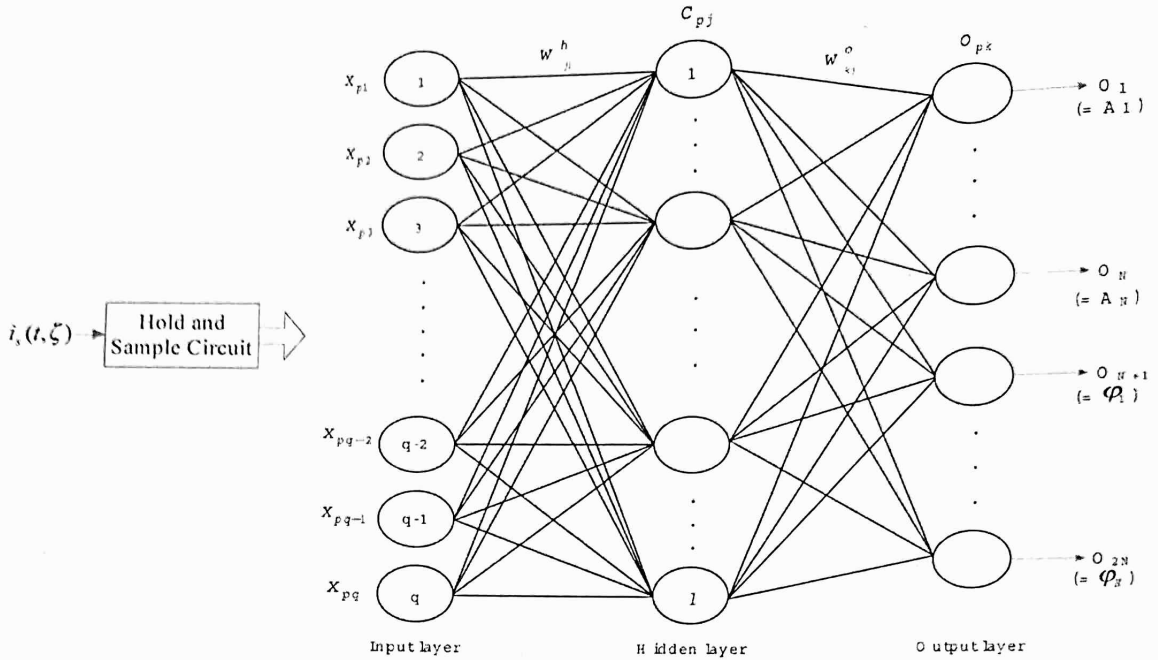


Fig. 1. The proposed ANN configuration.

achieved or no considerations in noise signal interference. All the above methods were not verified in practice. For example, the first published work using neural network for estimation of harmonic components in a power system was introduced by Osowski [14]. It stated that the relative error, at the highest noise, for all harmonic magnitudes was kept below 5%. However, the measured wave used a very simple waveform that contained only the fundamental, third, and fifth harmonics with one phase-shift considered. As a result, the difficulty arises when this approach is desired to be delivered into practical applications. Another work using a neural network for harmonic distortion analysis was introduced by Keerthipala *et al.* [16]. Even their scheme detected harmonic components within the tolerance limit of 5%, it only confirmed the effectiveness of harmonic identification to the seventh harmonics (350 Hz) under the simulated environment. This paper extends the Lin's work and presents a neural network-based algorithm that can identify both in magnitude and phase up to the eleventh harmonics (550 Hz) [20], [21]. It uses a systematic method for value determination of key model parameters even involving the noise environments. Experimental results have testified its performance with a variety of generated harmonics data under various real-time speed drive operations. Comparison with the conventional DFT method is also presented to demonstrate its very fast response and high accuracy.

II. HARMONIC DETECTION FORMATION AND SOLUTION

The line current signal is periodic with random magnitudes and phases under different nonlinear loads so that the distorted source current can be expressed as

$$i_s(t, \zeta) = \sum_{n=1,2,3,\dots}^N \sqrt{2}i_{sn}(\zeta) \sin(n\omega t + \varphi_n(\zeta)) \quad (1)$$

where i_{sn} , φ_n and ζ are root-mean-square (r.m.s.) magnitude, phase angle, and a random variable of the distorted source current (expressed in Fourier series), respectively.

With $i_s(t, \zeta)$ as the input source current to the hold and sample circuit in Fig. 1, the m th sampled output sequence is

$$i_s(m, \zeta) = \sum_{n=1,2,3,\dots}^N \sqrt{2}i_{sn}(m, \zeta) \sin(nm\theta + \varphi_n(\zeta)) \quad (2)$$

where $\theta = \omega T$ and T is the sample time period.

Let

$$x_p = [x_{p1}, x_{p2}, \dots, x_{pq}] \triangleq [i_s(1, \zeta), i_s(2, \zeta), \dots, i_s(q, \zeta)] \quad (3)$$

where the subscript "p" refers to the p th training vector, and "q" refers to the q th input unit.

An error function δ_{pk} for the k th output unit is defined as

$$\delta_{pk} \triangleq d_{pk} - o_{pk} \quad (4)$$

where d_{pk} is the object output (desired waveform composed of magnitude A_n and phase φ_n of harmonic components), and o_{pk} is the actual output from the k th unit.

The mean-square error function is defined as follows [5], [14], [17], [19]–[22]:

$$E_p \triangleq \frac{1}{2} \sum_{k=1}^{2N} \delta_{pk}^2. \quad (5)$$

To determine the direction in which to change the weights, the negative of the gradient of E_p , ∇E_p , is calculated with respect to the weights, w_{kj} based on the gradient steepest descent method for optimal solution [5], [6], [14], [17], [19]–[22]. Then, the values of the weights can be adjusted such that the total error

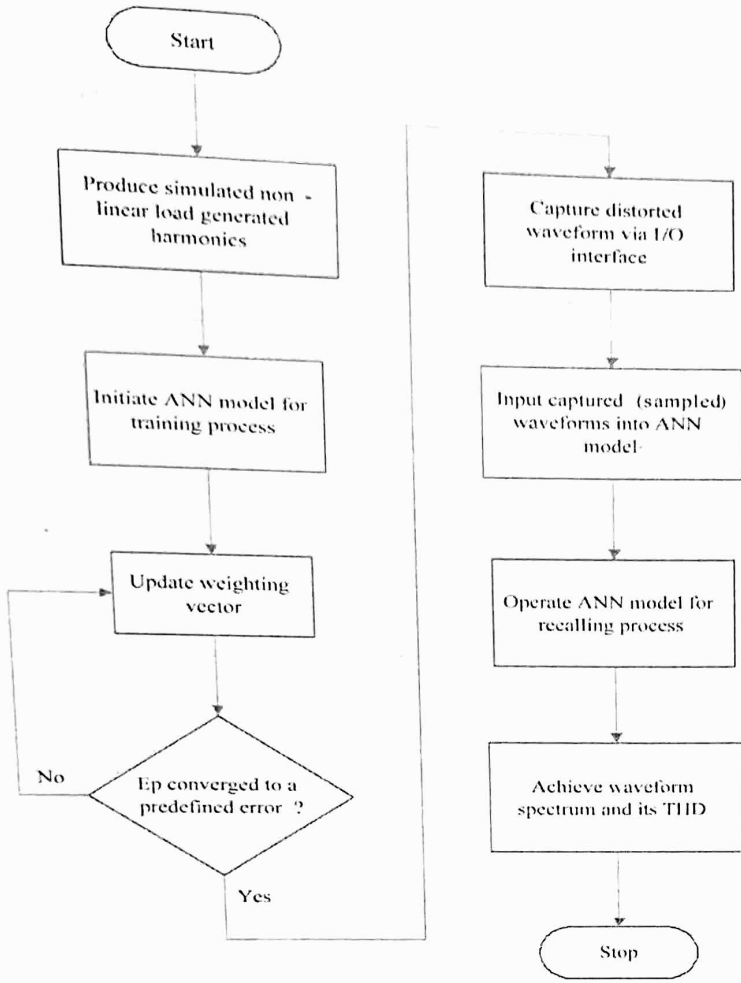


Fig. 2. Flowchart of the proposed ANN scheme.

is reduced. Detailed discussion of the control algorithm is given as Sections III–V.

III. PROPOSED HARMONIC DETECTION SYSTEM, CIRCUIT, AND ALGORITHM

A. Description of Overall Picture

There are two stages, i.e., training and recalling process, are required to implement the proposed artificial neural network (ANN) model. The flowchart of the ANN model is shown in Fig. 2. In the training stage, the simulated nonlinear load generated harmonics were initially produced in order to represent general possible distorted source current waveforms in the power line, shown as the following equation

$$i_s(t, \zeta) = \sum_{n=1,2,3,\dots}^N \sqrt{2}i_{sn}(\zeta) \sin(n\omega t + \varphi_n(\zeta)) + A_{\text{noise}} \sin(n_{\text{noise}}\omega t + \varphi_{\text{noise}}) \quad (6)$$

where A_{noise} is the magnitude of the noise signal, n_{noise} is its frequency component using a random noninteger value, and φ_{noise} is the phase of the noise signal.

For a set of simulated datas (sampled points of the distorted waveform in half cycle) in the first training (learning) process, there is a corresponding set of output “target” values that are the magnitude and phase coefficients of harmonics already stored in a data array. The initial weights (w_{ji}^h, w_{kj}^o) and bias values (θ_j^h, θ_k^o) referred to (7) and (10) and were randomized between

−0.5 and +0.5. When the neural network started learning, the output values were compared with the target values in a sequential manner. The weights were updated step by step according to the back propagation algorithm rule. The error between the actual outputs and the target values were forwarded to the input nodes, and then weights were adjusted to reduce the error after every update. The training process ceases, while the error is converged just below the predefined small bound (say 0.05). The updated weights obtained finally are the optimal values.

Once the offline training process is done, the source current waveform from the power line is captured via A/D conversion and I/O interface. Only 1/2 cycle of the distorted waveform is sampled and input into the ANN model for online recalling process using the well-trained neural network straightly away, i.e., no further training needed. Consequently, both harmonic magnitude and phase (output neurons) can be fast worked out directly in this stage.

B. Details of Experimental Implementation

The hardware system that is required to perform the ANN model is shown in Fig. 3. It is designed for an active I/O data access with a hardware interrupt function, and acts as a real-time dynamic waveform acquisition system. The waveform captured from the current sensor is very small (mV) so that it must be amplified hundreds of times by the amplifier before input to the hold and sample circuit, as well as the comparator. The A/D converter is connected to the PC and communicates with each other via the I/O interface channel. The zero-crossing detector is to generate an interrupt signal to the PC to ensure that the captured waveform starts from the zero-point of every cycle. The response time of this hardware system takes less than 0.01 ms. Main facilities (modules) for the hardware circuit are listed in Table I.

The proposed ANN model was implemented using Turbo C programming. The relevant procedures are presented in the order in which they were used during training for a single training-vector pair at Part (1). Part (2) presents the recalling process of the proposed system.

Part (1): Training process.

- Initialize the model parameters. Details are presented in Table II.
- Apply the input vector, $x_p = [x_{p1}, x_{p2}, \dots, x_{pq}]$ to the input units.
- Calculate the net-input values to the hidden layer units

$$\text{net}_{pj}^h = \sum_{i=1}^q w_{ji}^h x_{pi} + \theta_j^h. \quad (7)$$

- Calculate the outputs from the hidden layer: The sigmoid function is defined as

$$f_j^h (\text{net}_{pj}^h) = \left(1 + e^{-\text{net}_{pj}^h}\right)^{-1}. \quad (8)$$

Therefore, the outputs can be obtained as

$$c_{pj} = f_j^h (\text{net}_{pj}^h). \quad (9)$$

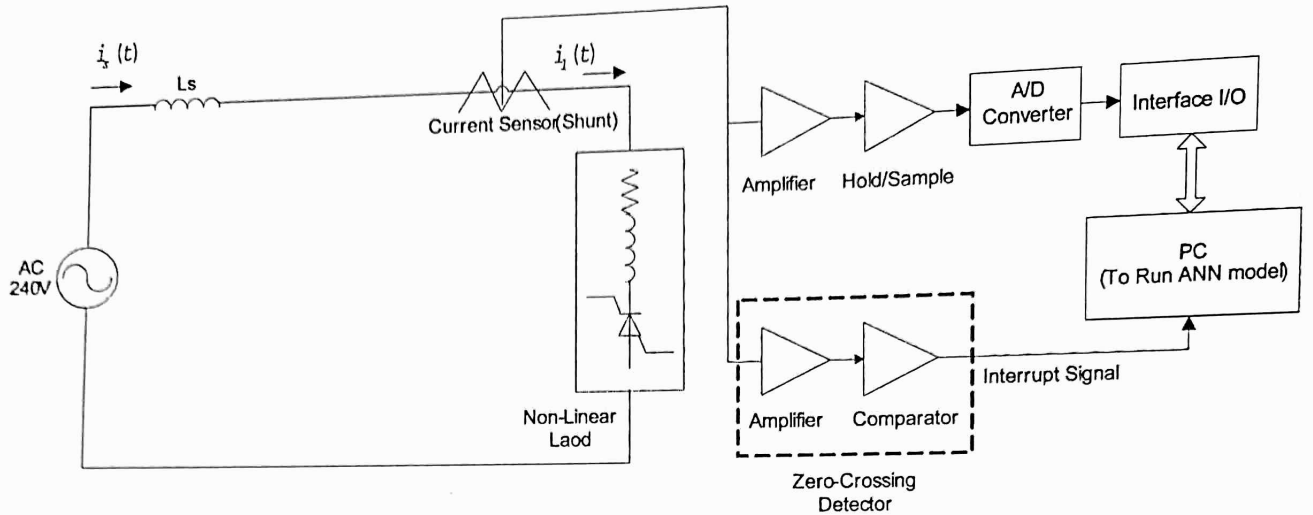


Fig. 3. Simplified system hardware circuit.

TABLE I
MAIN FACILITIES (MODULES) FOR THE HARDWARE CIRCUIT

Item Num.	Instrument Name	Specifications
1	Non-Linear Load	DC converter & DC variable-speed motor R.P.M.: 1450 HP: 4.5 Volts: 240 Amp.: 17.6
2	Shunt	Current sensor
3	Amplifier	Non-inverter amplifier (IC LM741)
4	Hold/Sample	Hold/Sample circuit (IC LF398)
5	Comparator	Comparator circuit (IC LM311N)
6	A/D Converter	A/D converter (IC ADC0804)
7	Interface I/O	Interface card (8255A&8259A)
8	PC	Pentium IV 1.8Ghz

- e) Move to the output layer. Calculate the net-input values to each unit

$$\text{net}_{pk}^o = \sum_{j=1}^{2N} w_{kj}^o c_{pj} + \theta_k^o. \quad (10)$$

- f) Calculate the outputs: Using the same sigmoid function as above, the outputs can be obtained as

$$o_{pk} = f_k^o (\text{net}_{pk}^o). \quad (11)$$

- g) Calculate the error terms for the output units

$$\delta_{pk}^o = (d_{pk} - o_{pk}) \frac{\partial f_k^o (\text{net}_{pk}^o)}{\partial (\text{net}_{pk}^o)}. \quad (12)$$

- h) Calculate the error terms for the hidden units

$$\delta_{pj}^h = \frac{\partial f_j^h (\text{net}_{pj}^h)}{\partial (\text{net}_{pj}^h)} \sum_k \delta_{pk}^o w_{kj}^o. \quad (13)$$

- i) Update the weights of the $(n+1)$ th iteration on the output layer

$$w_{kj}^o(n+1) = w_{kj}^o(n) + \alpha \Delta w_{kj}^o(n-1) + \eta \delta_{pk}^o c_{pj} + \Omega. \quad (14)$$

- j) Update the weights of the $(n+1)$ th iteration on the hidden layer

$$w_{ji}^h(n+1) = w_{ji}^h(n) + \alpha \Delta w_{ji}^h(n-1) + \eta \delta_{pj}^h x_i + \Omega. \quad (15)$$

- k) Repeat b)–j) until the network converges to an acceptable solution, i.e., $E_p \leq \varepsilon$, where ε is a predefined small value [21], [22].

Part (2): Recalling process.

- a) Apply the input vector (sampled source current waveform) to the input units.
- b) Calculate the output units (harmonic magnitudes and phases) employing the trained weights directly. No additional training process is required in this stage.
- c) Repeat a)–b) if there is a new input vector loaded.

This ANN configuration shown in Fig. 1 has 40 input neurons, receiving 40 sampled points of the distorted current waveform (50 Hz) in 1/2 cycle, i.e., each point sampled in every 0.25 ms, and producing the output neurons that represent the harmonic amplitudes and phases up to the eleventh harmonic components, i.e., six output neurons for magnitudes and six output neurons for phases. There is one hidden layer that uses 19 neurons to bridge the input layer and output layer. Therefore, the number of weight vectors is calculated by Num. of sampled points \times Num. of hidden vector + Num. of hidden vector \times Num. of output vector, i.e., $40 \times 19 + 19 \times 12 = 988$. The determination of input neurons number and the hidden layer is aimed to converge the network and reach satisfactory solution, i.e., $E_p \leq \varepsilon$ [20], [21]. Note that the complexity of the circuit is directly proportional to the number of input neurons though lower training errors, say 0.01, using more input neurons and hidden layer number may be achieved. The learning rate (η) and momentum value (α) are

TABLE II
IMPLEMENTATION PARAMETERS OF THE PROPOSED PACKAGE

Number of training patterns	350	Sampled points (q) of selected training & testing signals	40
Number of testing patterns	1400	Number of output vector (2N)	12
Number of hidden vector (l)	19	θ_j^h, θ_k^o (for initial values)	random
Number of hidden layer	1	w_{ji}^h, w_{kj}^o (for initial values)	random
Number of synaptic weight vector (w_{ji})	988	Ω	random
η	0.665	Number of training cycles	400
α	0.65		

set as 0.665 and 0.65, respectively. The initial synaptic weights, i.e., w_{ji}^h, w_{kj}^o , and the bias values, i.e., θ_j^h, θ_k^o are random numbers (≤ 0.1). The random momentum Ω is a random number set as ≤ 0.1 . The criteria used for choosing the number of parameters shown in Table II are derived from the desired performance evaluation given in the (5). There are only 350 training patterns employed in the training process, but up to 1400 testing patterns are used to verify the ANN model to be well trained. Number of training cycles is set as 400 to achieve the satisfactory low training error. The determination of the key factors (η and α) in the proposed model is discussed in Section III-B1.

1) *Practical Discussions of η , α and Global Minimum:* Selection of a value for the learning rate parameter, η , has a significant effect on the network performance. Usually, η must be a small number—on the order of 0.05 to 0.25—to ensure that the network will settle to a solution. However, a small value of η will have to make a large number of iterations. Increasing η as the network error decreases will speed convergence, but the network may bounce around too far from the actual minimum value if η gets too large. Consequently, the momentum α is added to increase the speed of convergence and keep the weight changes going in the same direction. However, η is affected by the selection of the momentum value (α) in the proposed model. We find that $\eta = 0.665$ and $\alpha = 0.65$ can approach a satisfactory solution. Sensitivity considerations between η and α are, thus, deduced in Section III-B2.

On the other hand, the gradient-descent search for the global minimum might accidentally find local minima instead of the global minimum. If the network stops learning before reaching an acceptable solution, a change in the number of hidden nodes can fix the problem. In the proposed system, we used the 19 hidden neurons and 1 hidden layer, which were experimentally found to be appropriate values. Another way can simply start over with a different set of initial weights. In this case, the solution is acceptable from an error standpoint, i.e., E_p , is set below 0.05, the minimum (solution) is near to global. Additionally, the random momentum Ω is added in (14) and (15) to help to avoid the network trapped in the local minimum [21], [22].

2) *Sensitivity Considerations:* With the developed ANN model, sensitivity studies are based on the analysis of testing pattern errors (E_p). Simulation results have been conducted to assess the two key model parameters, i.e., η and α , to achieve the optimal solution. In Fig. 4, the learning rate (η) ranged from 0.165 to 0.965, step in 0.1, was chosen to test the proposed model but the momentum term (α) was set 0.65. It was found

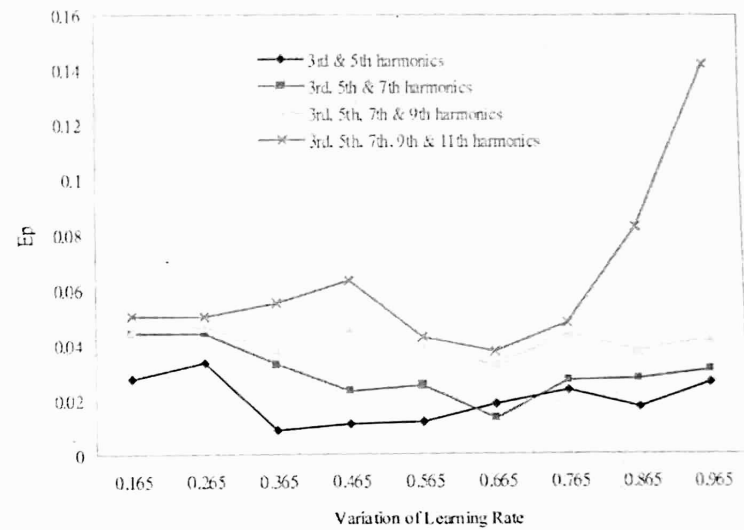


Fig. 4. E_p errors over variation of learning rate (η).

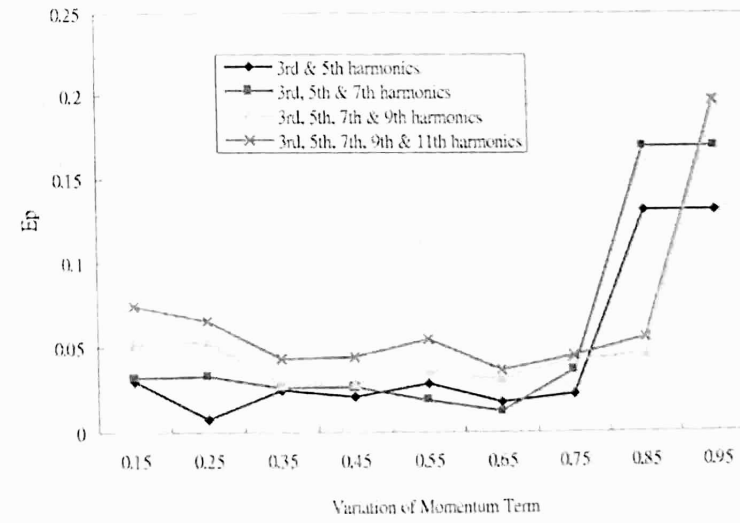


Fig. 5. E_p errors over variation of momentum term (α).

that the testing patterns with higher harmonic components showed higher E_p generally. Moreover, the E_p approached towards the acceptable minimum point, i.e., $\eta = 0.665$, in all cases. In addition, the η beyond 0.865 was not appropriate for the case of waveforms that contained up to the eleventh harmonics due to steeply high E_p occurring.

The E_p over various E_p from 0.15 to 0.95, step 0.1, is shown in Fig. 5 as η was set 0.665. As can be seen, the acceptable minimum location approached towards $\alpha = 0.65$ in all cases. I

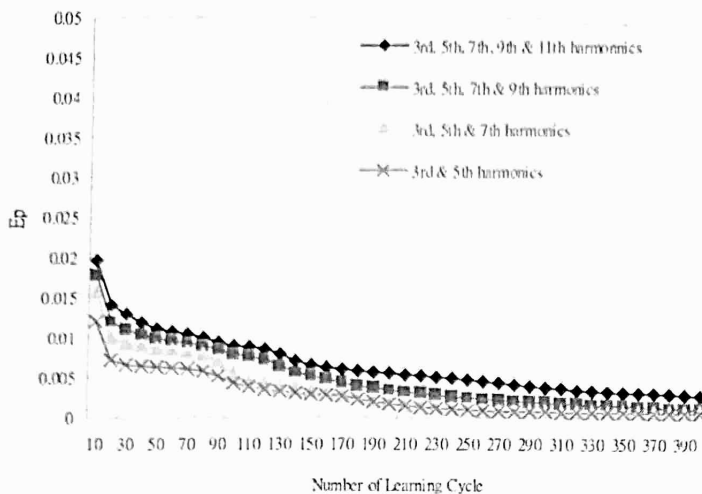


Fig. 6. Magnitude training E_p error curves with no noise signals.

was also found that the α beyond 0.85 was not appropriate for harmonic analysis due to intolerant E_p .

IV. DEMONSTRATION OF HARMONIC DETECTION RESULTS UNDER SIMULATION ENVIRONMENT

A. Detecting Harmonic Magnitude With No Noise Signals

Since the distorted waveforms consisting of odd harmonics are well known to cause the most adverse effects on power system applications, the testing waveforms that contained odd order harmonics such as third, fifth, and up to eleventh harmonic components were employed for testing with the trained ANN model. A total of 1400 testing patterns were generated with different (random) magnitude and phase angle properties that should represent possible power line distortions, according to the (1).

To test the generalizing capabilities of the magnitude networks, the distorted waveforms that contained odd harmonics up to the eleventh harmonic with no noises added were considered for the training process. As in the above conclusion in Section III, the learning rate (η) and the momentum term were set as 0.665 and 0.65, respectively. It was observed that the training was converged fast within 400 epochs, shown as Fig. 6. It also revealed that the initial training stages showed slightly higher errors curves and slower convergent speed in the training waveforms containing higher harmonics but achieved smooth curves in all cases η .

The pattern sum of squared error (E_p) was plotted for each set of testing waveforms in Fig. 7. The testing waveforms that contained the third, fifth, and up to the eleventh harmonics produced very low E_p errors, i.e., no more than 0.0167 in every case.

B. Detecting Harmonic Phase With No Noise Signals

With no noise signals, training E_p error curves for harmonic phase detection were shown In Fig. 8. These curves presented both fast and smooth convergence. After 1400 testing patterns

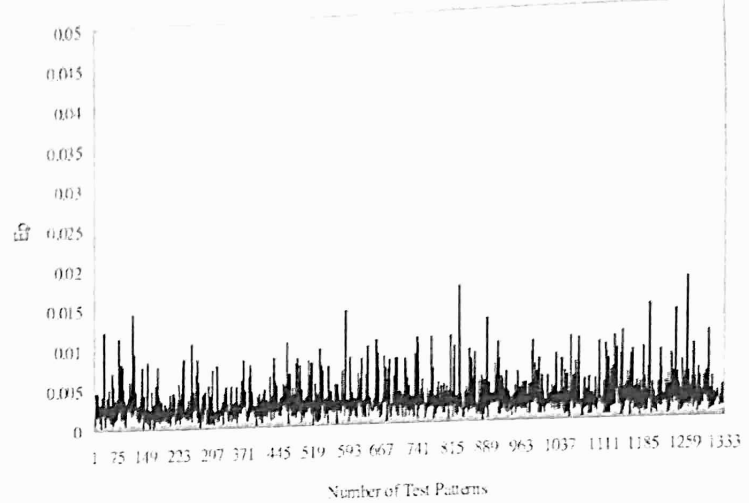


Fig. 7. Magnitude results using testing waveforms with no noise signals.

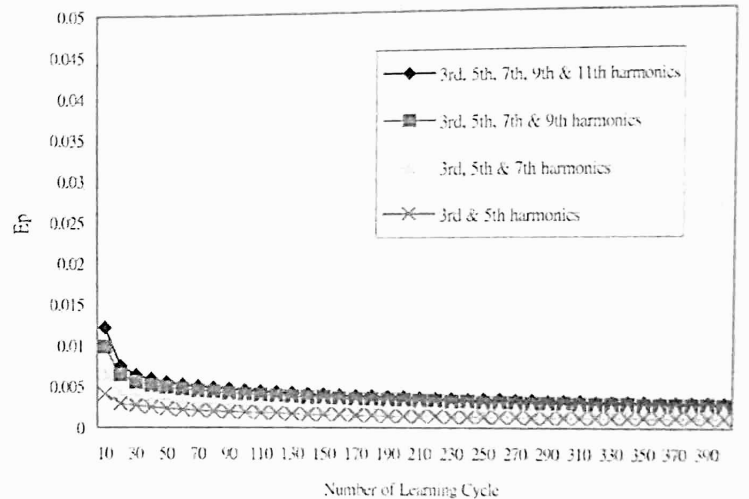


Fig. 8. Phase training E_p error curves with no noise signals.

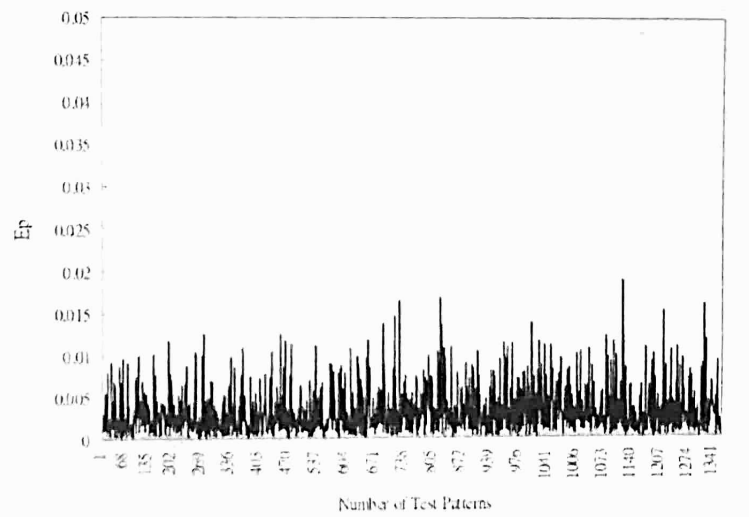


Fig. 9. Phase results using testing waveforms with no noise signals.

input to the trained ANN model, their phase results were obtained, as shown in Fig. 9. It can be seen that no E_p was beyond 0.0187.

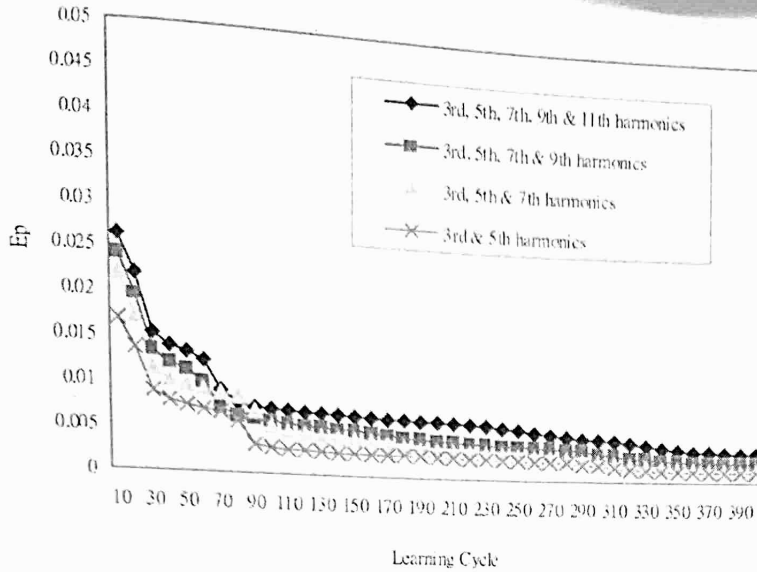


Fig. 10. Magnitude training E_p error curves with noise signals.

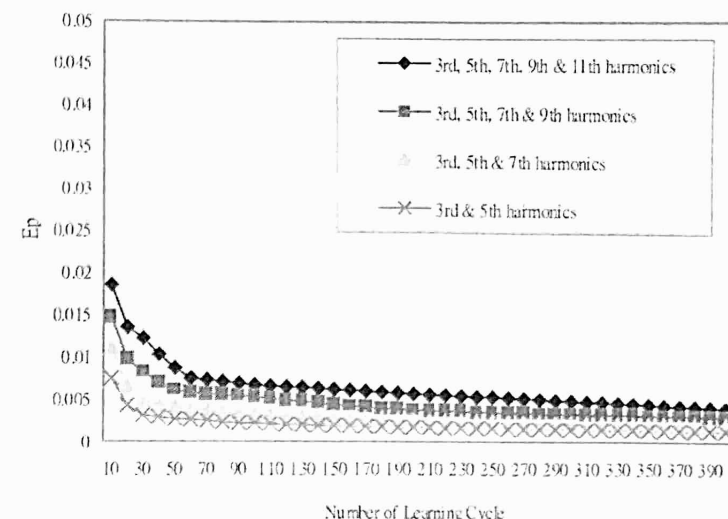


Fig. 12. Phase training E_p error curves with noise signals.

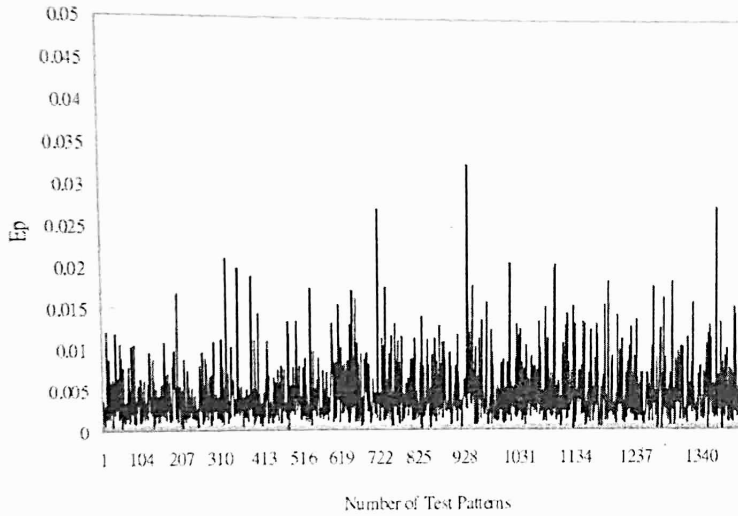


Fig. 11. Magnitude results using testing waveforms with noise signals.

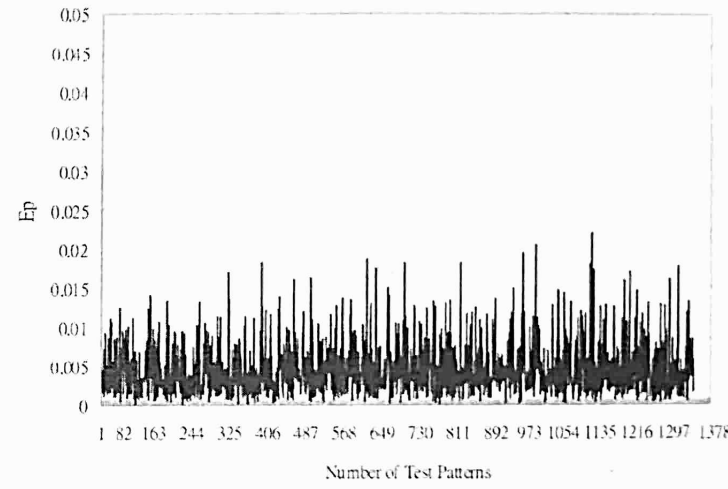


Fig. 13. Phase results using testing waveforms with noise signals.

C. Detecting Harmonic Magnitude With Noise Signals

In order to test the tolerance of harmonic detection network, a set of random noise signals shown in the (6) were generated and added in the 1400 testing patterns. These noises magnitudes are ranged as $-0.1 - +0.1$ and phases are ranged as $0^\circ - 360^\circ$, that may appear in general cases in power systems. The learning rate (η) and the momentum term were set as 0.665 and 0.65, respectively. Fig. 10 shows the training E_p errors curves using training samples with noise signals. Their convergent curves were similar to Fig. 6 but slightly higher in various testing waveforms. The results for the testing patterns that contained up to the fifth, seventh, ninth, and eleventh harmonics in noisy environments are shown in Fig. 11. Its corresponding maximum error value is 0.0325. It revealed that the E_p errors of testing patterns is a little higher than the case with no noises but still well within the tolerance limit (5%) in spite of the presence of noises.

D. Detecting Harmonic Phase With Noise Signals

With noise signals, training E_p error curves for harmonic phase detection were shown in Fig. 12. These curves also presented both fast and smooth convergence but slightly higher than the cases with no noises. Their phase results using 1400 testing

patterns were obtained, as shown in Fig. 13. As can be seen, no E_p was beyond 0.0247 in every case.

V. EXPERIMENTAL RESULTS USING ONLINE REAL-TIME DATA AND COMPARISON WITH DFT

The total harmonic distortion (THD) factor is the ratio of the r.m.s. value of all the harmonic components together to the r.m.s. amplitude of the fundamental component as following definition:

$$\text{THD}(\%) \triangleq \frac{\sqrt{i_s^2 - i_{s1}^2}}{i_{s1}} \times 100\% \\ = \frac{\sqrt{\sum_{n=2}^{\infty} i_{sn}^2}}{i_{s1}} \times 100\% = \frac{i_h}{i_{s1}} \times 100\%. \quad (16)$$

The proposed scheme has testified its harmonic detection in the distorted source current waveforms generated by the variable DC machine driving speeds at a wide range (100–1000 RPM) in the real-time implementation. For example, the source current waveform at 400 RPM was shown in Fig. 14. As can be seen in Fig. 15, its adverse harmonics mainly consisted of third and fifth components, and the THD was up to 51.73%. In

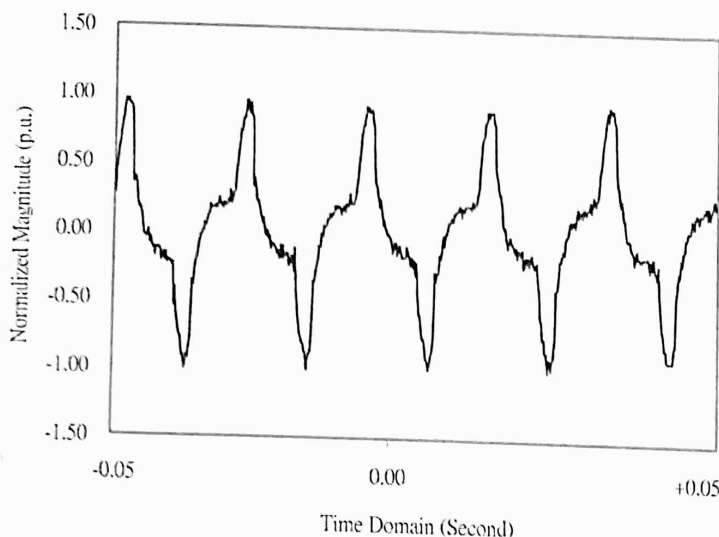


Fig. 14. Source current at 400 RPM.

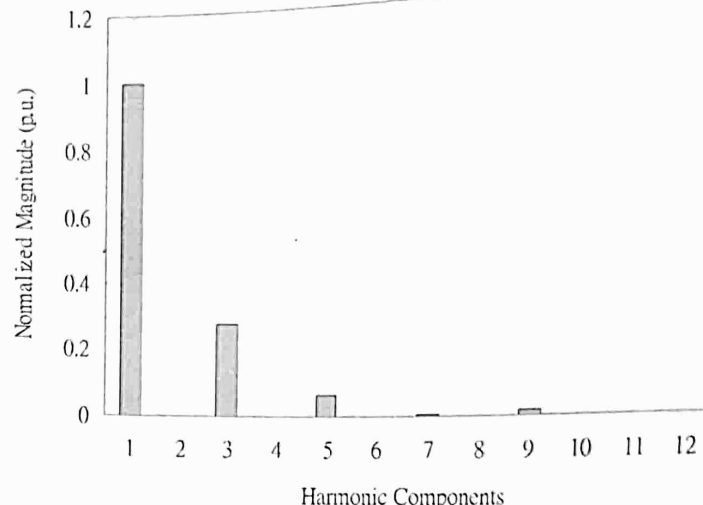


Fig. 17. Harmonic detection using the proposed scheme at 1000 RPM.

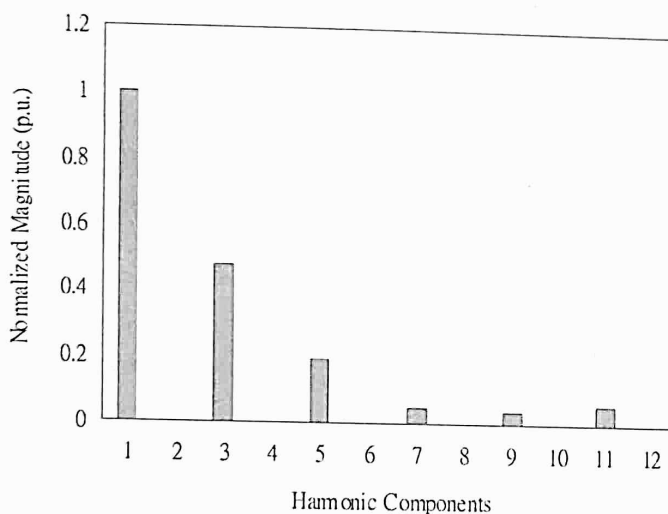


Fig. 15. Harmonic detection using the proposed scheme at 400 RPM.

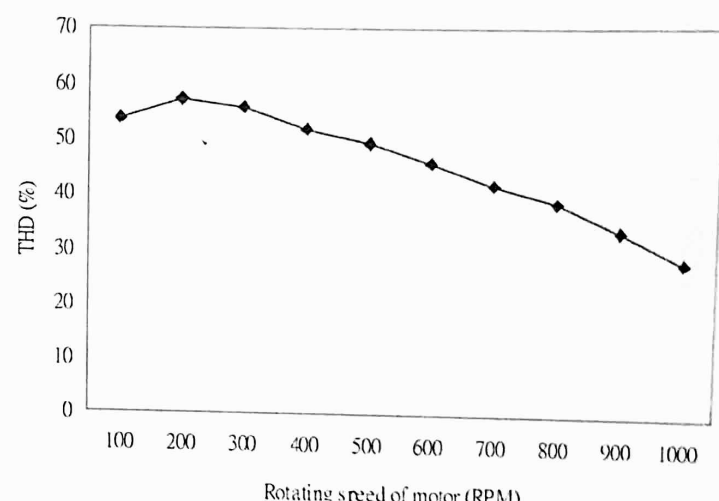


Fig. 18. Relative THD graph over various motor RPM.

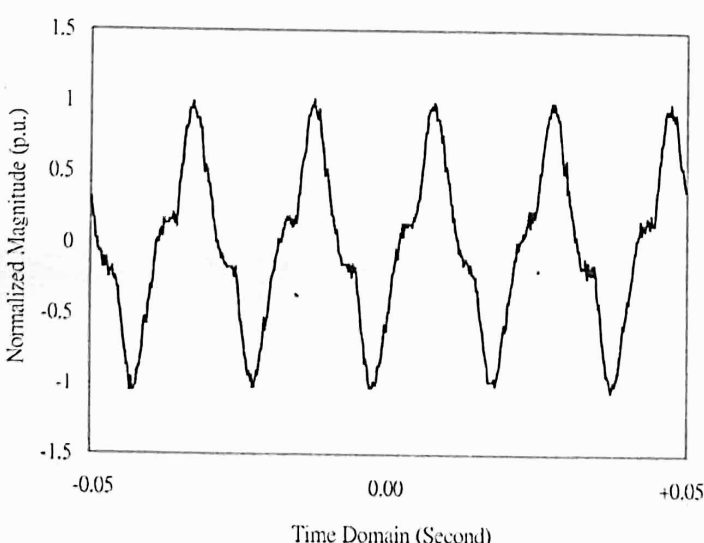


Fig. 16. Source current at 1000 RPM.

Fig. 16, the source current waveform, running at 1000 RPM, was closer to a pure sinusoid waveform due to no adverse harmonics existing and its harmonic components were shown in Fig. 17. Clearly, its THD was decreased in this case significantly, down

to 28.12%. There were ten line source currents measured under the DC variable-speed motor from 100 to 1000 RPM, shown in Fig. 18. It was found that the load generally produced higher line source current pollution in the power main at the lower speed. This explains why low speeds of operation are of great concern to electrical power system engineers.

Tables III and IV gave an overall comparison between the proposed ANN and DFT in harmonic magnitude and phase, respectively. These results demonstrated that the proposed ANN model coincided DFT method within less than 5% difference. Note that the fundamental magnitude component was normalized by both ANN and DFT.

VI. CONCLUSION

Harmonics contamination to the power line is getting serious in power systems whenever a large number of nonlinear loads are inevitable to be used in industry. Therefore, efficient and fast detection of harmonics has become an important issue in the electrical field. In this paper, a functional neural network model has been successfully developed for detecting harmonics of the power line distorted waveforms. Several hundred distorted current waveforms including noise cases were employed to train

TABLE III
RESULTS OF DETECTING HARMONICS MAGNITUDE

Harmonic RPM \	1 st		3 rd		5 th		7 th		9 th		11 th	
	ANN	DFT	ANN	DFT	ANN	DFT	ANN	DFT	ANN	DFT	ANN	DFT
100	1.00	1.00	0.475	0.468	0.209	0.215	0.123	0.127	0.064	0.065	0.033	0.034
200	1.00	1.00	0.486	0.493	0.250	0.246	0.122	0.121	0.047	0.047	0.024	0.024
300	1.00	1.00	0.510	0.497	0.230	0.235	0.090	0.091	0.016	0.017	0.046	0.045
400	1.00	1.00	0.496	0.481	0.190	0.190	0.044	0.045	0.040	0.038	0.058	0.056
500	1.00	1.00	0.472	0.464	0.159	0.155	0.010	0.011	0.045	0.046	0.045	0.047
600	1.00	1.00	0.435	0.433	0.114	0.113	0.017	0.017	0.056	0.058	0.031	0.032
700	1.00	1.00	0.398	0.408	0.089	0.092	0.023	0.024	0.040	0.041	0.023	0.022
800	1.00	1.00	0.381	0.373	0.075	0.076	0.025	0.026	0.037	0.038	0.009	0.009
900	1.00	1.00	0.321	0.328	0.060	0.060	0.026	0.026	0.023	0.024	0.004	0.004
1000	1.00	1.00	0.270	0.277	0.062	0.064	0.008	0.008	0.020	0.020	0.002	0.002

TABLE IV
RESULTS OF DETECTING HARMONICS PHASE (DEGREE °)

Harmonic RPM \	1 st		3 rd		5 th		7 th		9 th		11 th	
	ANN	DFT	ANN	DFT								
100	202.16	195.29	148.43	154.49	147.55	139.14	129.96	134.79	117.12	112.13	63.41	66.76
200	351.23	356.11	271.62	287.36	232.13	241.68	186.36	195.50	149.59	143.30	23.65	24.84
300	336.54	349.56	286.89	273.01	210.41	218.71	178.11	170.38	52.33	50.50	283.63	298.76
400	172.76	165.31	90.92	87.87	33.74	35.20	324.26	337.06	158.83	151.99	93.33	89.37
500	153.38	160.14	79.10	76.17	22.66	21.23	352.54	340.41	103.19	100.17	54.46	52.85
600	191.36	185.87	156.07	158.16	170.83	161.70	327.27	339.52	336.93	350.02	346.20	354.12
700	345.15	331.88	229.43	239.56	180.17	189.21	265.32	266.35	241.28	235.06	190.56	195.37
800	41.20	43.09	94.81	99.11	203.46	210.20	57.30	55.49	183.72	190.17	260.44	266.85
900	58.38	55.43	146.17	140.36	290.76	304.03	176.40	170.42	319.26	324.88	125.62	128.26
1000	54.81	57.24	145.05	151.38	328.25	340.46	205.21	196.69	38.53	40.04	20.83	21.68

the network. The trained ANN model was tested for 1400 patterns that contained up to the eleventh harmonics. It has been shown that the proposed model performed well in the tolerance of 5%. Furthermore, the testing results in noise environments that FFT (DFT) cannot work out accurately revealed that this model was tolerant for a practical level of noise (10%–20% of signal strength). As the conventional FFT requires more than two cycles to detect component of harmonics, the proposed approach needs only 1/2 of the distorted wave as the input signal. Therefore, it can improve the performance of harmonic compensation more than four times for the harmonic detector in active

power filters. Experimental results with real-time detection have confirmed that the proposed model was also well performed in practice. In addition, overall comparison with DFT validated it suitable for accurate harmonics detection applications. For future research work, this ANN model is recommended to be advanced for online dynamic harmonics filtering between harmonic loads and power networks.

REFERENCES

- [1] J. F. Chicharo and T. S. Ng, "Gradient-based adaptive IIR notch filtering for frequency estimation," *IEEE Trans. Acoust. Speech Signal Process.*, vol. 38, no. 5, pp. 769–777, May 1990.

- [2] T. T. Nguyen, "Parametric harmonic analysis," in *Proc. Inst. Elect. Eng.-Gen. Transm. Distrib.*, 1997, vol. 144, no. 1, pp. 21–25.
- [3] V. L. Pham and K. P. Wong, "Wavelet-transform-based algorithm for harmonic analysis of power system waveforms," *Proc. Inst. Elect. Eng.-Gen. Transm. Distrib.*, vol. 146, no. 3, pp. 249–254, 1999.
- [4] J. H. Marks and T. C. Green, "Predictive transient-following control of shunt and series active power filters," *IEEE Trans. Power Electron.*, vol. 17, no. 4, pp. 574–584, 2002.
- [5] M. Rukonuzzaman and M. Nakaoka, "Single-phase shunt active power filter with novel harmonic detection," in *Proc. Inst. Elect. Eng.-Electric Power Applications*, Jul. 2002, vol. 1, pp. 343–350.
- [6] F. Liu, Y. Zou, and K. Ding, "A novel real-time adaptive algorithm for harmonic detecting," in *Proc. 29th IEEE Annu. Conf. (IECON)*, Nov. 2003, vol. 3, pp. 2561–2565.
- [7] H. Akagi, "Trends in active power line conditioners," *IEEE Trans. Power Electron.*, vol. 9, no. 3, pp. 263–268, May 1994.
- [8] S. Valivaita and S. J. Ovaska, "Delayless method to generate current reference for active filters," *IEEE Trans. Power Electron.*, vol. 45, no. 4, pp. 559–567, Aug. 1998.
- [9] B. Oran, *The Fast Fourier Transform*. Englewood Cliffs, NJ: Prentice-Hall, 1974, pp. 140–146.
- [10] A. L. Paul and F. Wolfgang, *Introductory Digital Signal Processing with Computer Applications*. New York: Wiley, 1994.
- [11] R. W. Ramirez, *The FFT-Fundamental and Concepts*. Englewood Cliffs, NJ: Prentice-Hall, 1985.
- [12] Y. T. Chan and J. B. Plant, "A parameter estimation approach to estimation of frequencies of sinusoids," *IEEE Trans. Acoust. Speech Signal Process.*, vol. 29, no. 2, pp. 214–219, Apr. 1981.
- [13] Y.-M. Chen and R. M. O'Connell, "Active power line conditioner with a neural network control," *IEEE Trans. Ind. Appl.*, vol. 33, no. 4, pp. 1131–1136, Jul./Aug. 1997.
- [14] S. Osowski, "Neural network for estimation of harmonic components in a power system," in *Proc. Inst. Elect. Eng.-Gen. Transm. Distrib.*, Mar. 1992, vol. 139, no. 2, pp. 129–135.
- [15] N. Pecharanin, M. Sone, and H. Mitsui, "An application of neural network for harmonic detection in active filter," in *Proc. IEEE Int. Conf. Neural Netw.*, Jul. 2, 1994, vol. 6, pp. 3756–3760.
- [16] W. W. L. Keerthipala, T. C. Low, and C. L. Tham, "An application of a back-propagation type neural network for harmonic distortion analysis," in *Proc. Int. Power Eng. Conf.*, Singapore, Mar. 1, 1995, pp. 501–506.
- [17] N. Pecharanin, H. Mitsui, and M. Sone, "Harmonic detection by using neural network," in *Proc. IEEE Int. Conf. Neural Netw.*, Australia, Dec. 1, 1995, vol. 2, pp. 923–926.
- [18] A. A. M. Zin, M. Rukonuzzaman, H. Shaibon, and K. I. Lo, "Neural network approach of harmonics detection," in *Proc. Int. Conf. Energy Manage. Power Delivery (EMPD)*, Singapore, Mar. 3–5, 1998, vol. 2, pp. 467–472.
- [19] M. Rukonuzzaman, A. A. M. Zin, H. Shaibon, and K. I. Lo, "An application of neural network in power system harmonic detection," in *Proc. IEEE World Congr. Comput. Intell.*, May 4–9, 1998, vol. 1, pp. 74–78.
- [20] H. C. Lin, "Dynamic power system harmonic detection using neural network," in *Proc. IEEE Int. Conf. Cybern. Intell. Syst. (CIS2004)*, Singapore, Dec. 1–3, 2004, pp. 756–761.
- [21] ———, "Intelligent neural network based adaptive power line conditioner for real-time harmonics filtering," *Proc. Inst. Elect. Eng.-Gen. Transm., Distribution*, vol. 151, no. 5, pp. 561–567, Sep. 2004.
- [22] H. C. Lin and C. S. Lee, "Enhanced FFT based parametric algorithm for simultaneous multiple harmonics analysis," *Proc. Inst. Elect. Eng.-Gen. Transm., Distrib.*, vol. 148, pp. 209–214, May 2001.



Hsiung Cheng Lin was born in Chang Hua, Taiwan, on September 3, 1962. He received the B.S. degree from National Taiwan Normal University, Taipei, in 1986, and the M.S. and Ph.D. degrees from Swinburne University of Technology, Melbourne, Australia, in 1995 and 2002, respectively.

His working experience included Lecturer and Associate Professor at the Chung Chou Institute of Technology, Chang Hua. He is currently a Professor at the Department of Automation Engineering, Chienkuo Technology University (CTU), Chang Hua. His special fields of interest include power electronics, neural network, network supervisory system, and adaptive filter design.

Dr. Lin received an Outstanding Teaching Award from CTU in 2005 and 2006, respectively. He was also nominated and included in the First Edition of *Who's Who in Asia 2007*.